Research Square

Preprints are preliminary reports that have not undergone peer review.
They should not be considered conclusive, used to inform clinical practice,
or referenced by the media as validated information.

Flexible polymer nanocomposite film of BiFeO 3 - MnFe 2 O 4 – PMMA for magnetoelectric device applications

Preethy Augustine

pritiroseaugustine@gmail.com

Christ College

Arun K. J

Sree Kerala Varma College

Research Article

Keywords: Multiferroic, BiFeO3, PMMA, magnetic, dielectric, magnetoelectric

Posted Date: November 13th, 2026

DOI: https://doi.org/10.21203/rs.3.rs-11149255/v1

License: This work is licensed under a Creative Commons Attribution 4.0 International License.
Read Full License

Additional Declarations: No competing interests reported.

Flexible polymer nanocomposite film of $BiFeO_3$ - $MnFe_2O_4$ – PMMA for magnetoelectric device applications

Preethy Augustine[a]*, Arun K.J[b]

[a]Department of Physics, Christ College, Irinjalakuda, India

[b]Department of Physics, Sree Kerala Varma College, Thrissur, India

Corresponding Author: pritiroseaugustine@gmail.com

Abstract

The electric, magnetic, and magnetoelectric characteristics of $BiFeO_3$ - $MnFe_2O_4$ - PMMA (BMFO - PMMA) nanocomposite films were examined using the solvent-casting approach. The films' structural examination was carried out using XRD, SEM, AFM, and FTIR spectroscopy, confirming the existence of $BiFeO_3$ and $MnFe_2O_4$ phases as well as the amorphous phase of PMMA. At room temperature, magnetoelectric coupling experiments show that the composite film is multiferroic, with considerable magnetoelectric coupling between $BiFeO_3$, $MnFe_2O_4$, and PMMA. The coupling coefficient of the ceramic-polymer composite film with increased concentration of nanoparticles measured is 52.22 mV/cmOe, which is lower than the ME coefficient of PMMA alone. At room temperature, the hysteresis loop validates the composite's ferromagnetic characteristic. Improvements include a significantly greater dielectric constant (67), a huge dielectric loss, and a modest increase in ac conductivity. These unique nanocomposites' dielectric characteristics, magnetoelectric coupling, and ferromagnetic properties at room temperature make them highly appealing for magnetoelectric device applications.

Key words: Multiferroic, $BiFeO_3$, PMMA, magnetic, dielectric, magnetoelectric

1. Introduction

Polymer multiferroic nanocomposites are well-suited for application in electronic devices because they have a high degree of flexibility and can be cast in film form [1]. Additionally, these polymer-based composites have several other advantages, such as minimizing leakage currents and dielectric loss, which prevent failures during operation [2,3]. The nanocomposites of this type are largely determined by how nanoparticles interact with the polymer matrix. Nanocomposite films made of polymers exhibit improved ME responses [3 – 5]

The PMMA (polymethyl methacrylate) polymer is one of the best insulating polymers. It has been reported that this polymer has dielectric constants and dielectric losses of 2.6 and 0.014 respectively, measured at 1 MHz. Nanocomposites can be made from this polymer due to its low dielectric loss. Nanocomposites synthesized from polymers are crucial to polymer nanotechnology. Few studies have been conducted on the electrical, magnetic, structural, vibrational, and microstructural properties of PMMA - $BiFeO_3$ nanocomposites. Ahlawat et al. have discussed the magnetic and dielectric properties of PMMA-BFO nanocomposites [6]. They reported that as the level of BFO in the composite increased, so did the magnetic and dielectric properties. However, these properties are not suitable for device applications. El Sayed et al. have reported the increased dielectric constant from 2.03 to 5.19 with very small dielectric loss by the incorporation of 1 wt% of BiFeO3 into PMMA matrix [7]. Sun et al. revealed the microwave shielding performance of the material had been improved by filling BFO nanoparticles in PMMA matrix [8]. The outcomes of the reported investigations, however, are insufficient for use in devices. As a result, more research into this nanocomposite is required. Ceramic composites can improve the properties of polymers, potentially leading to a wide range of practical uses based on the filler in the polymer matrix [9 –14]. For the manufacture of polymer nanocomposites, solvent casting is one of the simplest and least time-consuming techniques. A large amount of research has been done on various polymer ceramic composites over the last few years [15,16]. Because of their use primarily in embedded capacitors, significant emphasis has been dedicated to the development of high dielectric constant polymer-ceramic composites. PMMA can be utilized as a matrix in nanocomposites because of its low dielectric loss.

The synthesis of $BiFeO_3$ – PMMA polymer nanocomposites and their structural, dielectric, and magnetic properties have been the subject of numerous studies. However, there has been no research into incorporating $BiFeO_3$ – $MnFe_2O_4$ (BFO - MFO) nanoparticles into a diamagnetic and insulating PMMA matrix. As a result, the current research describes the synthesis of $BiFeO_3$ – $MnFe_2O_4$ – PMMA (BMFO - PMMA) polymer nanocomposites as well as their structural, electrical, magnetic, and magnetoelectric coupling properties.

2. Experimental procedure

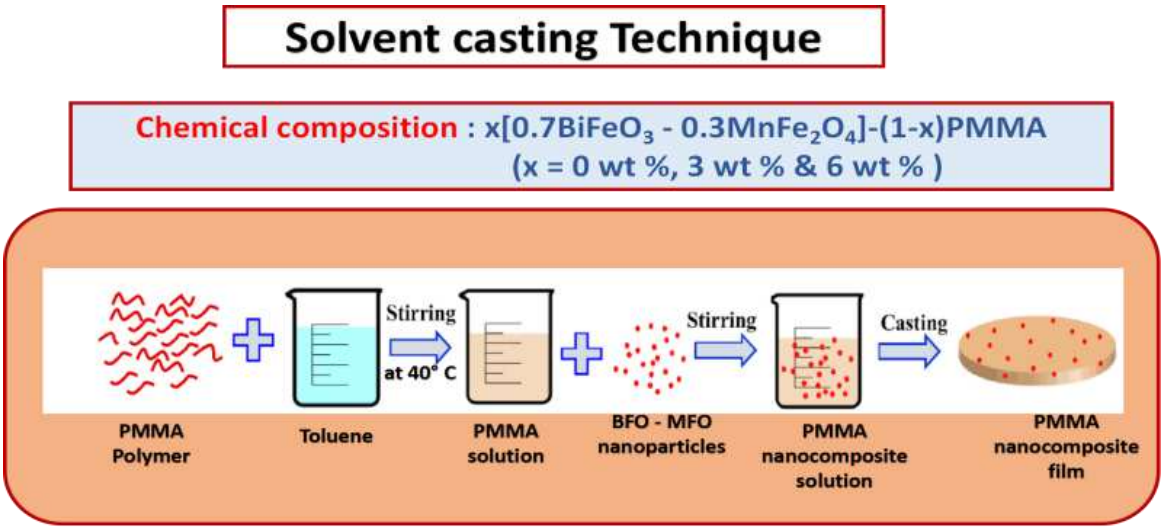


Figure 1. Schematic representation of $BiFeO_3$ - $MnFe_2O_4$ - PMMA nanocomposite films

Initially, the Pechini method was used to synthesize $0.7BiFeO_3$ - $0.3MnFe_2O_4$ ceramic powder [17]. $x[0.7BiFeO_3\text{-}0.3MnFe_2O_4]$ - (1 - x) PMMA films for x = 0, 3 wt%, 6 wt% were prepared by the solvent casting technique. Toluene was used as a solvent to make the PMMA solution. PMMA was weighed and mixed with the solvent toluene and stirred for an hour at 40ºC. And then, different weight percentages of nanoparticles were added to the solution and stirred for 24 hours to make PMMA nanocomposite solution. The solution mixtures were then cast on a clean petridish and allowed to dry for three days at room temperature. A thin polymeric film was created once the solvent had completely evaporated.

The crystalline nature of BFO – MFO - PMMA nanocomposites was examined using Rigaku Miniflex 600 X – ray Diffractometer. The 2θ values from 20° - 80° was scanned at the

rate of 3°/ min. The FT-IR absorption spectra of all the composites were recorded using ThermoFisher scientific Fourier Transform Infrared (FT-IR) spectrometer. The SEM images of the samples were captured using Carl Zeiss Sigma Field Emission Scanning Electron Microscopy (FE-SEM). The magnetization measurements were carried out using Vibrating Sample Magnetometer (VSM) in the field range of 20 kOe ≥ H ≥ -20 kOe. Radiant's precision multiferroic testing system was used for the examination of ferroelectric properties of the samples. The frequency-dependent dielectric parameters in the range 100 Hz to 2 MHz were measured using an Impedance Analyzer (Agilent E4980). The ME coupling coefficient measurement of the composites were performed at fixed H_{ac} = 10 Oe of frequency 850 Hz collinearly with varying H_{dc} from 0 – 5 kOe and at fixed H_{dc} of 1 kOe collinearly with varying H_{ac} from 0 – 80 Oe. A lock-in amplifier set up was used to record the induced ME voltage. All the characterization studies were executed at room temperature.

3. Results and discussion

3.1 XRD analysis

The XRD pattern of x[0.7$BiFeO_3$ - 0.3$MnFe_2O_4$] - (1 - x) PMMA nanocomposites for (x= 0 wt%, 3 wt%, 6 wt%) at room temperature is shown in Figure 2. The figure also includes an XRD graph of the 0.7$BiFeO_3$ - 0.3$MnFe_2O_4$ nanoparticles. The existence of an amorphous polymeric chain is responsible for the emergence of a broad peak between 10º-20º, while all of the acute peaks are caused by BFO – MFO nanoparticles. $BiFeO_3$ and $MnFe_2O_4$ are the peaks designated by the letters B and M, respectively. The strength and sharpness of the peaks grow as the loading percentage of BFO - MFO nanoparticles increases, as seen in the Figure 2.

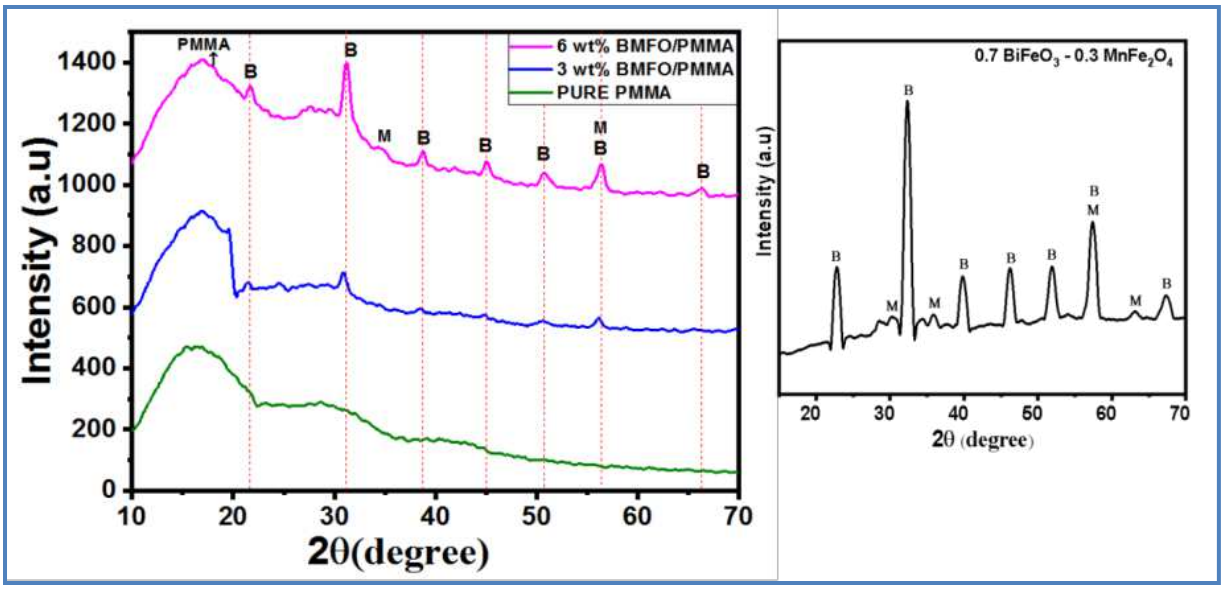


Figure 2. XRD pattern of x[0.7$BiFeO_3$-0.3$MnFe_2O_4$] - (1-x) PMMA nanocomposites (x = 0 wt%, 3 wt%, 6 wt%.

3.2 FESEM analysis

The FESEM images of pristine PMMA, 3 wt% BMFO/PMMA, and 6 wt% BMFO/PMMA nanocomposites are displayed in Figure 3. As seen in the Figure 3, the BMFO nanoparticles are simply dispersed in the PMMA matrix. The pristine PMMA has a uniform morphology. With the addition of BMFO particles, however, the PMMA matrix displayed variable dispersion and a slight aggregation of nanoparticles. It could be owing to the matrix's fast evaporation of solvent. As can be observed in the image, the agglomeration has grown as the loading percentage of the nanoparticles has increased. It is because of the interfacial interaction and load transfer between the matrix and the nanoparticles.

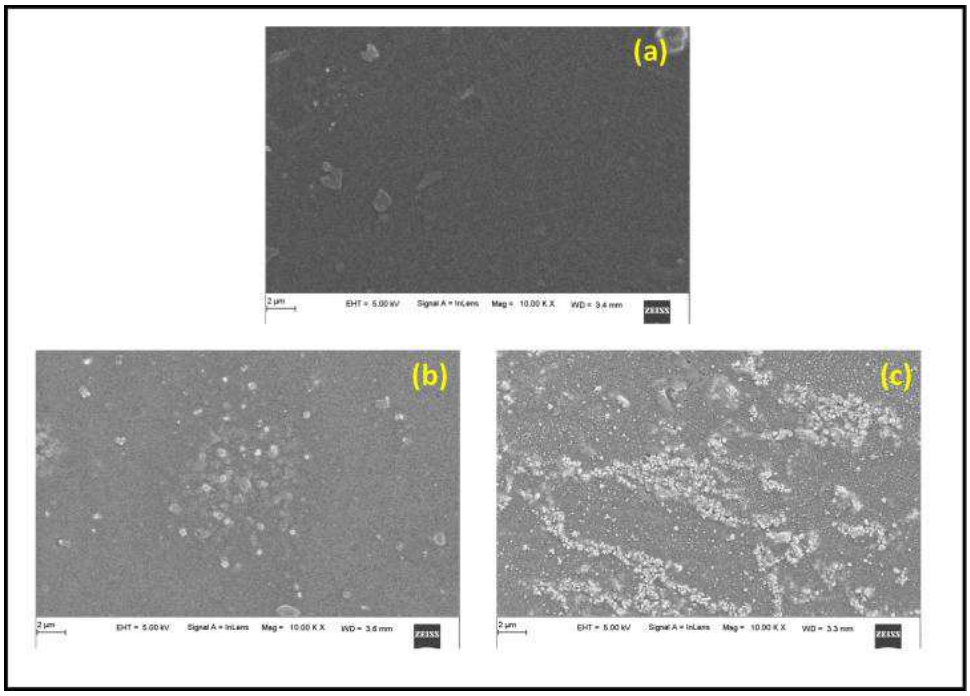


Figure 3. FESEM of x[0.7$BiFeO_3$-0.3$MnFe_2O_4$] - (1-x)PMMA nanocomposites (x= 0 wt%, 3 wt%, 6 wt%)

3.3 FTIR analysis

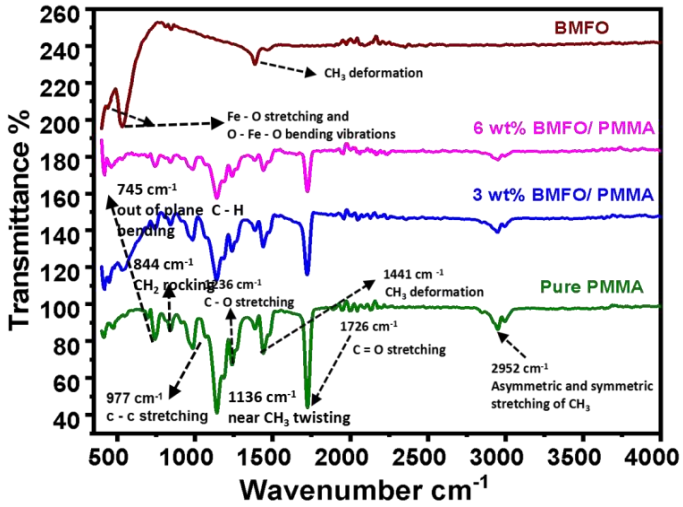


Figure 4. FTIR spectra of x[0.7$BiFeO_3$-0.3$MnFe_2O_4$] - (1-x) PMMA nanocomposites (x= 0 wt%, 3 wt%, 6 wt%)

The FTIR spectra of pristine, 3 wt% BMFO/PMMA and 6 wt% BMFO/PMMA nanocomposites are depicted in Figure 4. The presence of a broad band at 2952 cm^{-1} resulted from the asymmetric and symmetric vibrations of the $–CH_3$, $–CH_2$ groups in PMMA molecules [18]. The ester carbonyl group stretching vibrations, C=O stretching, caused a sudden intensity peak at 1726 cm^{-1} [19]. C–H bending vibrations cause a band at 1441 cm^{-1}. C-O-C symmetrical stretching vibrations are related to the peak at 1136 cm^{-1} [20]. The Fe-O stretching and O-Fe-O bending vibrations, which are characteristic of the octahedral FeO_6 groups in perovskite compounds, are responsible for two significant absorption peaks of about 549.75 and 439.80 cm^{-1}[21]. Peak vibrations at 977 cm^{-1}, 844cm^{-1}, and 745cm^{-1} are caused by C-C stretching, C-CH_2 twisting, and C-H bending [7], respectively.

3.4 AFM analysis

The AFM images of x [0.7$BiFeO_3$ - 0.3$MnFe_2O_4$] - (1- x)PMMA nanocomposites for (x = 0 wt%, 3 wt%, 6wt%) in 2D and 3D are shown in Figure 5 (a), (b), and (c), and 5 (d), (e) & (f), respectively. The 2D and 3D photos of the x = 0 composition show rough surface topography, whereas the surface roughness of other compositions reduces as x increases. It means that as the percentage of BFMO nanoparticles in the polymer matrix was increased, the overall roughness of the films decreased. It could be owing to the polymer and nanoparticles' intermolecular, intermolecular, and interfacial interactions. The black area represents the amorphous phase, the brown area represents the crystalline phase, and the white and yellow areas represent fully and partially embedded nanoparticles. With the dispersion of nanoparticles into the polymer PMMA, the film could acquire a crystalline phase. It also improves the smoothness of the films. Here the roughness values for x = 0, 3, and 6 wt% are shown at 7.91 nm, 6.52 nm, and 6.35 nm, respectively.

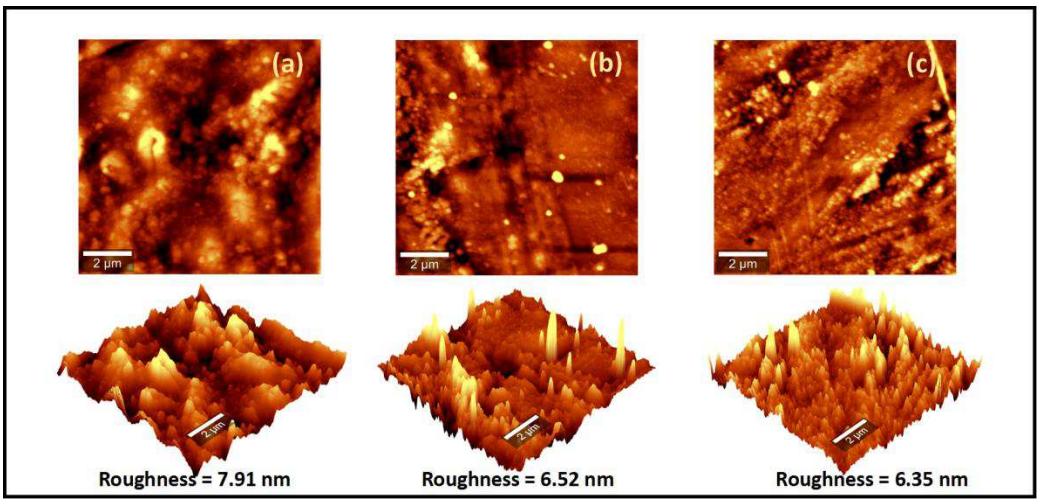


Figure 5 (a), (b) & (c) AFM images of x[0.7$BiFeO_3$-0.3$MnFe_2O_4$] - (1-x)PMMA nanocomposites (x = 0 wt%, 3 wt%, 6 wt%) in 2D and **(d), (e) & (f)** AFM of x[0.7$BiFeO_3$-0.3$MnFe_2O_4$] - (1-x)PMMA nanocomposites (x = 0 wt%, 3 wt%, 6wt%) in 3D.

3.5 Magnetic properties

Magnetization (M) versus applied field (H) for x [0.7$BiFeO_3$ - 0.3$MnFe_2O_4$] - (1-x) PMMA nanocomposites (x = 0 wt%, 3 wt%, 6 wt%) measured using VSM at room temperature is shown in Figure 6. The M-H curve shows zero susceptibility, which indicates diamagnetic behaviour [6]. These composite films exhibit an increase in magnetization when the percentage of BFMO nanoparticles rises to 6 wt%, as expected. The values of magnetic parameters are summarized in Table 1. It has been shown that M_s, M_r and H_c increases linearly when the magnetic nanoparticles in the nanocomposites increase. For 0, 3, and 6 wt% loading of BFMO nanoparticles, the saturation magnetization (M_s) values are 0.085, 0.318, and 0. 545 emu/cm^3. The squareness ratio ($M_r/M_s < 0.5$) [22] verifies the multi - domain structure of the composites. Moreover, the samples show a tendency to become magnetically harder, as can be seen from the high value of coercivity [23], after incorporating BMFO nanoparticles into the PMMA matrix.

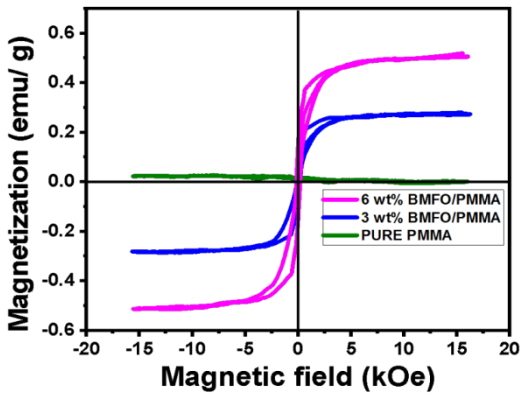


Figure 6. M – H loop of x[0.7$BiFeO_3$ - 0.3$MnFe_2O_4$] - (1 - x)PMMA nanocomposites (x = 0 wt%, 3 wt%, 6 wt%)

Table 1 Magnetic parameters of x[0.7$BiFeO_3$ - 0.3$MnFe_2O_4$] - (1 - x)PMMA nanocomposites

Samples	M_s (emu/g)	M_r (emu/g)	M_r/ M_s	H_c (Oe)
X = 0	0.0858	.00355	0.0414	169.37
X = 3 %	0.3183	0.0846	0.2657	199.20
X = 6 %	0.5454	0.1538	0.2820	200.27

3.6 Dielectric properties

The dielectric constant of x [0.7$BiFeO_3$ - 0.3$MnFe_2O_4$] - (1 - x) PMMA nanocomposites at room temperature is shown in Figure 7(a) for (x = 0 wt%, 3 wt%, and 6 wt%). As it is observed, the dielectric constant of the polymer composites rises as the concentration of the BMFO increases over all the frequency ranges. The dielectric constant also declines as the frequency increases. This decreasing trend could be observed in the very low frequency region, below 100 Hz in PMMA – BFO - MFO composites. It becomes constant-frequency independent above 100 Hz. The value of the dielectric constant that is observed is 64 for the 6 wt% BMFO/PMMA composites. Therefore, the enhancement of dielectric constant is found with the incorporation of BMFO nanoparticles. It results from the interfacial polarization among ceramic-polymer interfaces [18]. Figure 7 (b) represents the dielectric loss of the polymer nanocomposites. The samples showed

greater dielectric loss than the polymer PMMA. These features matched well with the earlier reported results, which could be related to the large loss of the loading of BMFO nanoparticles. Also shown in Figure 7 (c) is the frequency-dependent ac conductivity of the polymer nanocomposites. Across the entire frequency range, the ac electrical conductivity of the composites rises with frequency, and it is only a little greater than the pure PMMA electrical conductivity, indicating that the nanocomposites have good insulating properties [24].

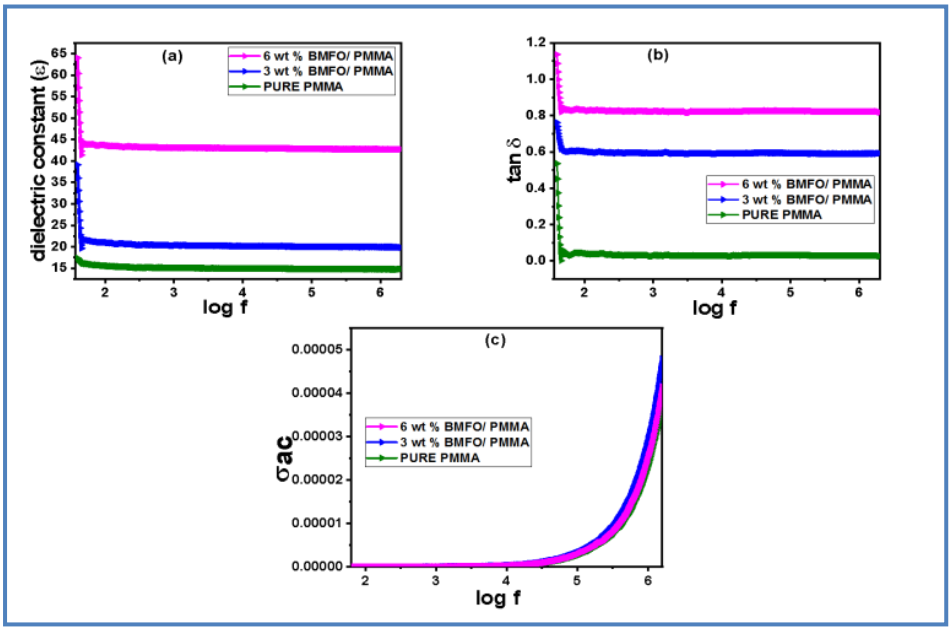


Figure 7. Frequency dependence dielectric parameters of x[0.7$BiFeO_3$ - 0.3$MnFe_2O_4$] - (1-x)PMMA nanocomposites (x= 0 wt%, 3 wt%, 6 wt%)

3.7 Ferroelectric properties

The ferroelectric performance of x [0.7$BiFeO_3$ - 0.3$MnFe_2O_4$] - (1 - x) PMMA nanocomposites for (x= 0 wt%, 3 wt%, 6 wt %) was analyzed by displaying the polarization (P) vs electric field (E) hysteresis loop. The Figure 8 represents the P - E loop of the polymer nanocomposite samples. The entire procedure was completed at RT within the range of an electric field of ±20V at a frequency 50Hz. P-E loops are symmetric about the origin, indicating that the electric dipoles are uniformly distributed inside the materials [25]. The ferroelectric parameters of PMMA and BMFO/ PMMA nanocomposites are listed in Table 2. For PMMA sample, the saturation polarization (P_m) and remanent polarization (P_r) are observed8.6561×10-^{5}μC/cm^2 and

$8.6885\times10^{-3}\mu C/cm^2$ respectively. But the value of P_m and P_r is found to be suppressed after the dispersion of BMFO nanoparticles in different weight percentages into the PMMA matrix. It may be due to the highly lossy nature of the BMFO particles.

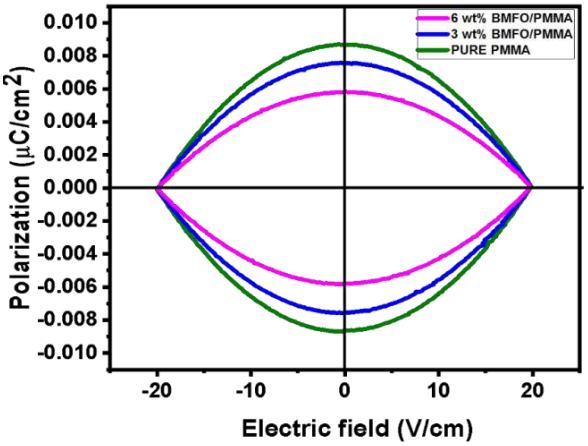


Figure 8. P – E loop of $x[0.7BiFeO_3 - 0.3MnFe_2O_4] - (1-x)$PMMA nanocomposites (x = 0 wt%, 3 wt%, 6 wt%)

Table 2 Ferroelectric parameters of $x[0.7BiFeO_3 - 0.3MnFe_2O_4] - (1 - x)$PMMA nanocomposites

Samples	P_{max} ($\mu C/cm^2$)	P_r ($\mu C/cm^2$)
X = 0%	8.6561×10^{-5}	8.6885×10^{-3}
X = 3%	8.4029×10^{-5}	7.5807×10^{-3}
X =6%	4.8427×10^{-5}	5.8162×10^{-3}

3.8 Magnetoelectric coupling analysis

The AC measurement of the composites' ME voltage is shown in Figure 9(a) by varying the AC magnetic field (H_{ac}) at 850 Hz from 0 to 80 Oe while maintaining a constant DC magnetic field of 1 kOe. The ME output voltage develops linearly as Hac is varied. Similar results are reported for many polymer nanocomposites [26, 27]. The slope of the magnetoelectric coupling curve determines the magnetoelectric coupling coefficient (α). The ME coupling coefficient of

the polymer PMMA is observed to be 78.58 mV/cmOe. The estimated values are summarized in Table 3. The results confirm the reduced ME voltage coefficient of BMFO/PMMA composites as compared to the polymer PMMA. It is because of the presence of conductive and lossy behaviour of the BMFO nanoparticles in the composite. The value of 'α' decreased as the loading percentage of the nanoparticles increased in the PMMA matrix. The ME voltage verses dc field (H_{dc}) from 0 – 5000 Oe at a constant H_{ac} of 10 Oe is shown in Figure 9(b). The coupling coefficient may be calculated by dividing the ME voltage by H_{ac}. The evaluated results match the results of the ac measurement.

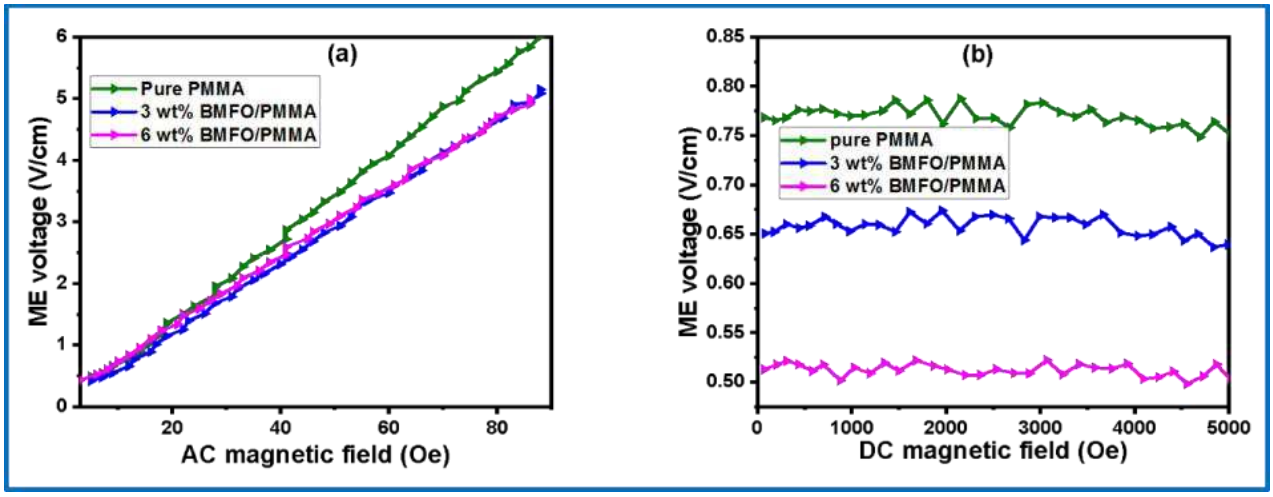


Figure 9. The variation of ME voltage with H_{ac} and H_{dc} of x[0.7$BiFeO_3$ - 0.3$MnFe_2O_4$] - (1-x)PMMA nanocomposites (x= 0 wt%, 3 wt%, 6 wt%)

Table 3 ME voltage coefficient of x[0.7$BiFeO_3$ - 0.3$MnFe_2O_4$] - (1 - x)PMMA nanocomposites

Samples	α (mV/cmOe)
X= 0 wt %	78.58
X= 3 wt%	67.39
X= 6 wt%	52.22

Conclusion

The $BiFeO_3$ - $MnFe_2O_4$ - PMMA (BMFO - PMMA) nanocomposite films were fabricated by the solvent-casting technique. As revealed by microstructural analysis, BMFO nanoparticles have been dispersed in a PMMA polymer matrix. Observations of magnetic hysteresis loops at room temperature show an increase in total magnetization with an increase of magnetic BMFO nanoparticles in the PMMA matrix. When comparing the nanocomposite film to the PMMA sample, it exhibits a significantly higher dielectric constant (67), a large dielectric loss, and a slight increase in ac conductivity. The ME coupling coefficient of the PMMA sample showed the highest value, and it decreased with the addition of BMFO nanoparticles due to its lossy nature. The results show that insulating PMMA (α = 78.58 mV/cmOe) is an effective polymer for controlling leakage current in the fabrication of ME devices.

Declarations

Availability of Data and Materials: All data supporting the findings of this study are included in the article and its Supplementary Information files.

Funding
The authors received no specific funding for this research or the preparation of this manuscript.

Ethics, Consent to Participate, and Consent to Publish declarations
Not applicable.

Competing Interests
The authors declare that they have no known competing financial interests or personal relationships that could have appeared to influence the work reported in this paper.

Acknowledgement
The authors are thankful to CIF, IIT Guwahati for VSM facility and DST Purse Lab, Mangalore University for FESEM characterization. The authors also acknowledge SAIF, Mahatma Gandhi University for providing AFM facility.

References

[1] P. Martins, C.M. Costa, M. Benelmekki, G. Botelho, S. Lanceros-Mendez, On the origin of the electroactive poly(vinylidene fluoride) β-phase nucleation by ferrite nanoparticles via surface electrostatic interactions, CrystEngComm. 14 (2012) 2807–2811.

[2] S. Jiansirisomboon, K. Songsiri, A. Watcharapasorn, T. Tunkasiri, Mechanical properties and crack growth behavior in poled ferroelectric PMN - PZT ceramics, Curr. Appl. Phys. 6 (2006) 299–302.

[3] S. Roy, R. Chatterjee, S.B. Majumder, Magnetoelectric coupling in sol-gel synthesized dilute magnetostrictive- piezoelectric composite thin films, J. Appl. Phys. 110 (2011) 3–6.

[4] K. Yano, A. Usuki, A. Okada, Synthesis and properties of polyimide-clay hybrid films, J. Polym. Sci. Part A Polym. Chem. 35 (1997) 2289–2294.

[5] R.P. Ummer, P. Sreekanth, B. Raneesh, R. Philip, D. Rouxel, S. Thomas, N. Kalarikkal, Electric, magnetic and optical limiting (short pulse and ultrafast) studies in phase pure (1 - x)$BiFeO_3$ - x$NaNbO_3$ multiferroic nanocomposite synthesized by the pechini method, RSC Adv. 5 (2015) 67157–67164.

[6] A. Ahlawat, S. Satapathy, S. Bhartiya, M.K. Singh, R.J. Choudhary, P.K. Gupta, $BiFeO_3$/poly(methyl methacrylate) nanocomposite films: A study on magnetic and dielectric properties, Appl. Phys. Lett. 104 (2014).

[7] A.M. El Sayed, Aspects of structural, optical properties, and relaxation in ($BiFeO_3$ or $NaTiO_3$) – PMMA: Hybrid films for dielectric applications, J. Phys. Chem. Solids. 148 (2021) 109767.

[8] X. Sun, Y.Q. Ma, Y.F. Xu, S.T. Xu, B.Q. Geng, Z.X. Dai, G.H. Zheng, Improved magnetic performance at low and high temperatures in non-exchange-coupling $CoFe_2O_4$/$CoFe_2$ nanocomposites, J. Alloys Compd. 645 (2015) 51–56.

[9] Y. Kojima, A. Usuki, M. Kawasumi, A. Okada, Y. Fukushima, T. Kurauchi, O. Kamigaito, Mechanical properties of nylon 6-clay hybrid, J. Mater. Res. 8 (1993) 1185–1189.

[10] P.B. Messersmith, E.P. Giannelis, Synthesis and barrier properties of poly(caprolactone)layered silicate nanocomposites, J. Polym. Sci. Part A Polym. Chem. 33 (1995) 1047–1057.

[11] M.A. Osman, V. Mittal, M. Morbidelli, U.W. Suter, Polyurethane adhesive nanocomposites as gas permeation barrier, Macromolecules. 36 (2003) 9851–9858.

[12] J. Liu, H. Deng, X. Zhai, T. Lin, X. Meng, Y. Zhang, W. Zhou, P. Yang, J. Chu, Influence of Zn doping on structural, optical and magnetic properties of $BiFeO_3$ films fabricated by

the sol-gel technique, Mater. Lett. 133 (2014) 49–52.

[13] S.F. Wang, H.B. Lv, X.S. Zhou, Y.Q. Fu, X.T. Zu, Magnetic nanocomposites through polyacrylamide gel route, Nanosci. Nanotechnol. Lett. 6 (2014) 758–771.

[14] Q. Tan, Q. Wang, Y. Liu, Magnetic properties and spontaneous polarization of La-, Mn- and N - doped tetragonal $BiFeO_3$: A first-principles study, Materials (Basel). 11 (2018) 17–19.

[15] M.A. Osman, V. Mittal, M. Morbidelli, U.W. Suter, Epoxy-layered silicate nanocomposites and their gas permeation properties, Macromolecules. 37 (2004) 7250–7257.

[16] A. Patsidis, G.C. Psarras, Dielectric behaviour and functionality of polymer matrix - Ceramic $BaTiO_3$ composites, Express Polym. Lett. 2 (2008) 718–726.

[17] P. Augustine, Y. Narayana, N. Kalarikkal, An effective strategy for the development of multiferroic composite nanostructures with enhanced magnetoelectric coupling performance: a perovskite–spinel approach, Nanoscale Adv. 3 (2021) 4866–4877.

[18] M.S. Tamboli, P.K. Palei, S.S. Patil, M. V. Kulkarni, N.N. Maldar, B.B. Kale, Polymethyl methacrylate (PMMA) - bismuth ferrite (BFO) nanocomposite: Low loss and high dielectric constant materials with perceptible magnetic properties, Dalt. Trans. 43 (2014) 13232–13241.

[19] M.K. Mishra, S. Moharana, B. Behera, R.N. Mahaling, Surface functionalization of $BiFeO_3$: A pathway for the enhancement of dielectric and electrical properties of poly (methyl methacrylate) – $BiFeO_3$ composite fi lms, (2017) 1–10.

[20] W. Luo, L. Zhu, N. Wang, H. Tang, M. Cao, Y. She, Efficient removal of organic pollutants with magnetic nanoscaled $BiFeO_3$ as a reusable heterogeneous fenton-like catalyst, Environ. Sci. Technol. 44 (2010) 1786–1791.

[21] C.N. Chinnasamy, A. Narayanasamy, N. Ponpandian, R. Justin Joseyphus, B. Jeyadevan, K. Tohji, K. Chattopadhyay, Grain size effect on the Néel temperature and magnetic properties of nanocrystalline $NiFe_2O_4$ spinel, J. Magn. Magn. Mater. 238 (2002) 281–287.

[22] P. Kaviraj, R. Pramanik, A. Arockiarajan, Influence of individual phases and temperature on properties of $CoFe_2O_4$ - $BaTiO_3$ magnetoelectric core-shell nanocomposites, Ceram. Int. 45 (2019) 12344–12352.

[23] M. Wang, X. Sun, B.Q. Geng, S.T. Zhang, Y.Q. Ma, Synthesis and magnetic properties of $CoFe_2/CoFe_2O_4$ nanoparticles diluted in the MgO matrix, Mater. Res. Bull. 95 (2017) 9–16.

[24] S. Acharya, J. Ray, T.U. Patro, P. Alegaonkar, S. Datar, Microwave absorption properties of reduced graphene oxide strontium hexaferrite/poly(methyl methacrylate) composites, Nanotechnology. 29 (2018).

[25] A. Raza Khan, G.M. Mustafa, S. Kumail Abbas, S. Atiq, M. Saleem, S.M. Ramay, S. Naseem, Flexible ferroelectric and magnetic orders in $BiFeO_3/MnFe_2O_4$ nanocomposites to steer wide range energy and data storage capability, Results Phys. 16 (2020) 102956.

[26] R.P. Ummer, R. Raneesh, C. Thevenot, D. Rouxel, S. Thomas, N. Kalarikkal, Electric, magnetic, piezoelectric and magnetoelectric studies of phase pure ($BiFeO_3$ - $NaNbO_3$) - (P(VDF-TrFE)) nanocomposite films prepared by spin coating, RSC Adv. 6 (2016) 28069–28080.

[27] N. Adhlakha, K.L. Yadav, M. Truccato, Manjusha, P. Rajak, A. Battiato, E. Vittone, Multiferroic and magnetoelectric properties of $BiFeO_3$ - $CoFe_2O_4$ - poly(vinylidene-flouride) composite films, Eur. Polym. J. 91 (2017) 100–110.